JOURNAL OF MATERIALS SCIENCE 25 (1990) 482–486

Non-isothermal crystallization kinetics of $Ag–As_2S_3$ semiconductor glasses

M. F. KOTKATA, C. S. MOHAMED, M. M. RADWAN
Physics Department, Faculty of Science, Ain Shams University, Cairo, Egypt

Using a differential thermal analysis technique to give single scan thermograms, the transformation mode, n, and the activation energy of crystallization, E, were determined for the chalcogenide glasses of the system $Ag_x(As_2S_3)_{100-x}$, with $x = 6$, 15 and 25. Both n and E were found to be compositionally dependent. The value of n varies between 2.1 and 3.6, and that of E between 2.4 and 3.6 eV. The crystallization kinetic data were explained using X-ray diffraction results of amorphous and crystalline structures.

1. Introduction

Non-isothermal analysis of the crystallization kinetics of chalcogenide semiconducting glasses has become increasingly attractive in comparison with isothermal techniques. Non-isothermal experiments can be performed over a shorter period and wider temperature range. Moreover, many phase transformations occur too rapidly to be measured under isothermal conditions because of the inherent transients associated with the experimental apparatus.

Many studies on thermally induced transformation in binary selenium-based glasses and in mixed stoichiometric chalcogenide binaries have been made using differential thermal analysis (DTA) and differential scanning calorimetry (DSC) [1–5]. In a previous study [6], some isothermal transformations in glasses of the system $Ag–As_2S_3$ have been investigated by following the changes in electrical conduction and X-ray diffraction. In the present report, a non-isothermal analysis of the crystallization kinetics of the same system is performed. A number of kinetic parameters have been evaluated from DTA measurements. The results obtained are linked to X-ray diffraction structure data from amorphous and crystallized samples.

2. Experimental procedures

The method of sample preparation is given in [6, 7]. DTA curves were obtained for each composition using a Shimazu DT-30 Thermal Analysis System. Powdered samples (25 mg) were weighed out from the bulk material and placed in aluminium sample holders for the DTA scans. To obtain conventional DTA curves for kinetic analysis using a single-scan technique [3], a slow constant scan-rate of $2°\,min^{-1}$ or less with a relatively high speed of the recorder chart were used. Details of the DTA experimental arrangement are given in [4].

3. Results and discussion

Figure 1 shows the exothermic peaks of the thermograms obtained for powder $Ag_x(As_2S_3)_{100-x}$ samples scanned at a rate of $2°\,min^{-1}$. Comparison of these exothermic peaks with those scanned at $10°\,min^{-1}$ (Fig. 2) shows that the single exothermic peak which appears for the sample of composition $Ag_6(As_2S_3)_{94}$ at the rate of $10°\,min^{-1}$ splits into two crystallization peaks at the lower rate of $2°\,min^{-1}$. This suggests that the single peak is a superposition of two peaks unresolved at the high scan rate. Also, the two crystallization peaks that appeared at a scanning rate ϕ of $10°\,min^{-1}$ for the composition $Ag_{25}(As_2S_3)_{75}$ are for the split into three peaks at the $2°\,min^{-1}$ scan rate.

Table I gives the estimated values of the begin-peak-end of the different crystallization exothermic peaks recorded at $\phi = 2°\,min^{-1}$ for the three compositions investigated and those at $10°\,min^{-1}$ are given in [7].

The volume fraction $\alpha(t)$ transformed after a given time t (or temperature T) can be calculated from the thermogram using the Borchard assumption [8]:

$$\alpha(t) = [(c_p/h)\Delta T + a(t)]/A \quad (1)$$

where c_p is the heat capacity of the sample (standard), h is the heat transfer coefficient for the sample (standard), ΔT is the temperature difference between the sample and standard, A is the total peak area between the ΔT-graph and the corrected base line, and $a(t)$ is a part of the area under the DTA curve up to the time t (or temperature T). In suitably arranged DTA-equipment, the value of c_p/h can be neglected [8, 9]

TABLE I The values of the begin-peak-end of the different crystallization exothermic peaks recorded at $\phi = 2°\,min^{-1}$ for the glasses $Ag_x(As_2S_3)_{100-x}$

Glass composition	T_c (°C) ($\phi = 2°\,min^{-1}$)		
	Begin	Peak	End
$Ag_6(As_2S_3)_{94}$	202	262	278
	281	312	350
$Ag_{15}(As_2S_3)_{85}$	190	213	228
	230	241	250
	252	267	273
$Ag_{25}(As_2S_3)_{75}$	204	222	238
	242	260	284
	296	312	320

0022–2461/90 $03.00 + .12

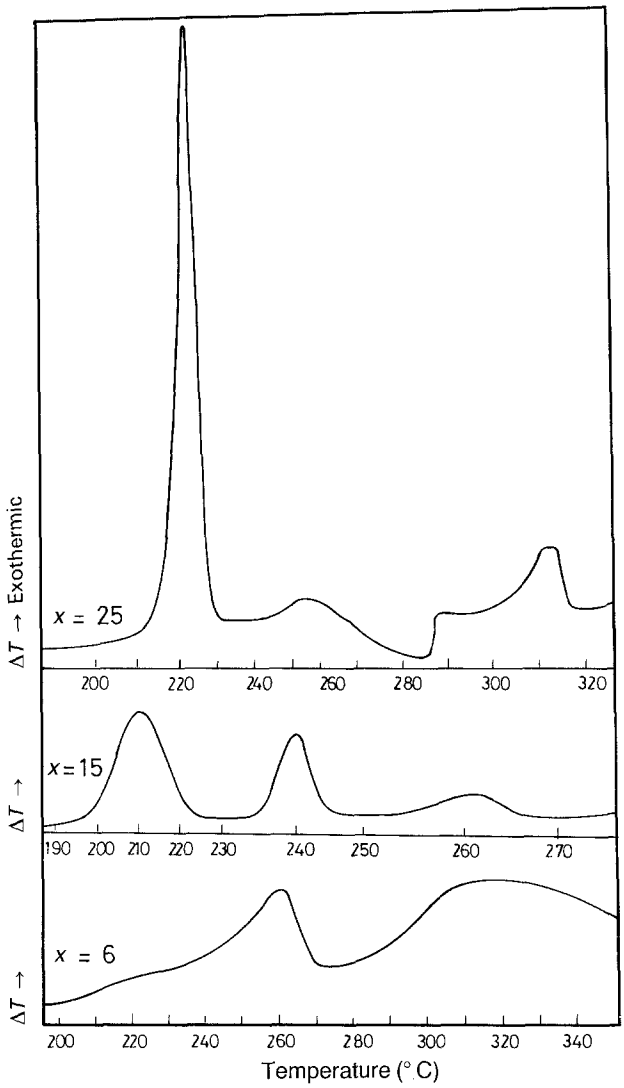

Figure 1 Exothermic crystallization peaks of the glasses $Ag_x(As_2S_3)_{100-x}$ as obtained from DTA scanned at $2°\,min^{-1}$.

and thus Equation 1 reads

$$\alpha(t) = a(t)/A \quad (2)$$

Thus, $\alpha(t)$ can be deduced by integrating the ΔT graph. Figure 3 shows the variation of $\alpha = f(t)$ for the three exotherms of the composition $Ag_{15}(As_2S_3)_{85}$ (as an example). Similar behaviour to that seen in Fig. 3 was obtained for each exotherm of the other two compositions. Such sigmoidal behaviour indicates an autocatalytic reaction as is often observed in various kinds of solid reaction [3–5].

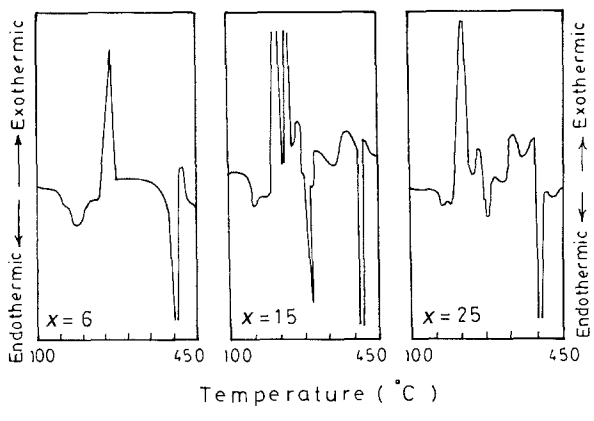

Figure 2 DTA thermograms of the glasses $Ag_x(As_2S_3)_{100-x}$. Heating rate is $10°\,min^{-1}$.

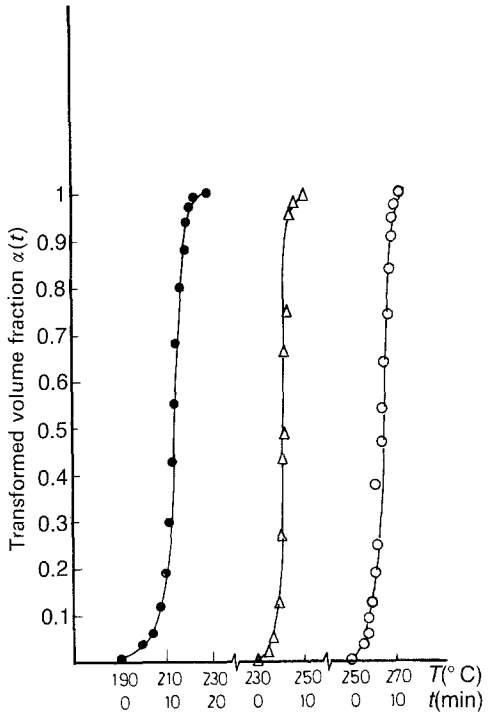

Figure 3 The temperature (and time) dependence of volume fraction of crystallization for glassy $Ag_{15}(As_2S_3)_{85}$.

An estimation of the complex activation energy of crystallization, E, can be made by using Piloyan's method [10]. This is based on the differential form of the model reaction for α, known as $g(\alpha)$, and on Borchard's assumption [8] that the reaction rate, $d\alpha/dt$, is proportional to the temperature deflection ΔT as detected by DTA. Details of the theoretical approach of the applied model are given in [3, 11]. Accordingly, the fractional volume transformed at any temperature is related to the kinetic parameters by the following equations

$$\log [g(\alpha)] = \log \left[\frac{K_0^{1/n} E}{\phi R}\right] - \frac{E}{2.303 nRT} \quad (3)$$

and

$$\ln [-\ln (1 - \alpha)] = n \ln \left[\frac{K_0^{1/n} E}{\phi R}\right] - \frac{E}{RT} \quad (4)$$

where K_0 is the pre-exponential factor of an Arrhenius equation defining the rate constant $K = K_0 \exp(-E/RT)$, and is considered to be constant with respect to temperature, n is a kinetic parameter known as the Avrami exponent which reflects the nucleation rate and/or the growth morphology, E is the activation energy of the process, R is the gas constant, and ϕ is the heating rate ($\phi = dT/dt$).

The effective activation energy E/n can be deduced, according to Equation 3, from the slope of a plot of $\log [g(\alpha)]$ versus $1/T$. This, of course, means that the function $g(\alpha)$ is evaluated for the most probable reaction mechanism. In Fig. 4, $\log [g(\alpha)]$ versus $1/T$ is plotted for the composition $Ag_6(As_2S_3)_{94}$ (as an example) for different kinetic equations [12]. These results indicate that the two functions $A_2(\alpha)$ and $A_3(\alpha)$ are valid for the largest range of α. However, a least-square fitting indicates that the function $A_3(\alpha)$, where $[-\ln (1 - \alpha)^{1/3} = Kt]$, almost covers the

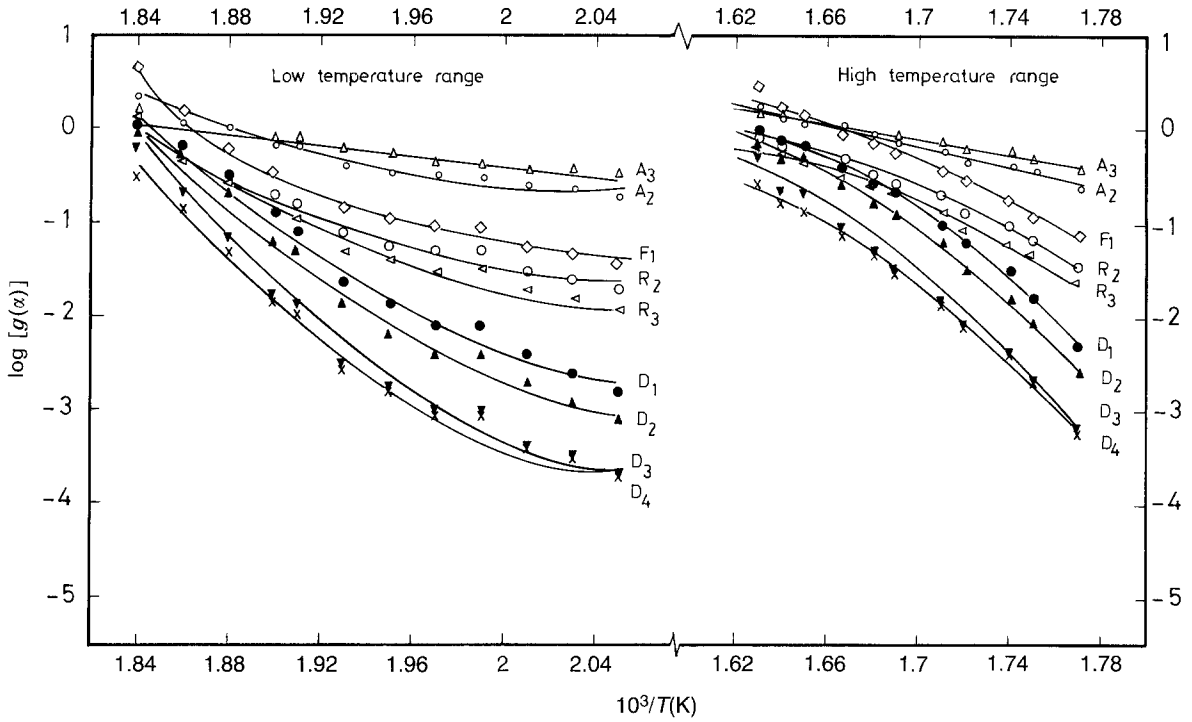

Figure 4 Plots of log [$g(\alpha)$] versus $1/T$ for the crystallization of $Ag_6(As_2S_3)_{94}$ calculated for various kinetic equations. The functions are labelled according to the symbols given in [12].

experimental calculations over the total range of α, $(0 < \alpha < 1)$.

Figure 5 shows the plots of log [$g(\alpha)$] versus $1/T$ for the rate controlling function $A_3(\alpha)$ of the other two compositions investigated. That is, the function $A_3(\alpha)$ is designated as the most probable one for the devitrification process of each exotherm in the three compositions investigated. Fitting can be achieved with other log [$g(\alpha)$] curves, but only in a narrow range of α.

It is worthwhile to emphasize that the accurate knowledge of E is essential for the determination of the Avrami exponent n. Least-square plots of $\ln[-\ln(1-\alpha)]$ versus $1/T$ for the investigated $Ag_x(As_2S_3)_{100-x}$ compositions are given in Fig. 6. These plots yield a straight-line relationship for the apparent exothermic peaks, Equation 4, the slope of each determining the value of E. Hence, the Avrami exponent n can be determined from the values of E/n and E.

The values of E and n are given in Table II together with the melting point values. Table II indicates that the high melting temperature of a phase corresponds to a high energy of crystallization of the same phase.

A study of the values of E shows a small difference for the first exothermic peak in the three compositions (2.45, 2.7 and 2.4 eV). This is explained when combined with the results of X-ray diffraction studies for the crystallized samples of the same compositions [6],

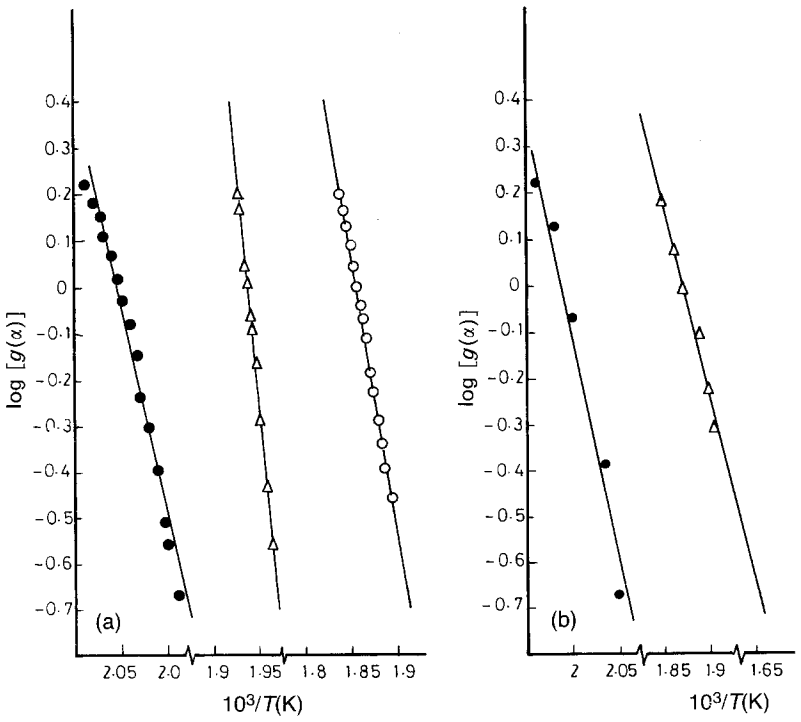

Figure 5 Plots of log [$g(\alpha)$] versus $1/T$ for the most probable reaction kinetic function $A_3(\alpha)$ of $Ag_x(As_2S_3)_{100-x}$, $x = 15$ (a) and $X = 25$ (b). (●) Low, (△) medium and (○) high temperature peaks.

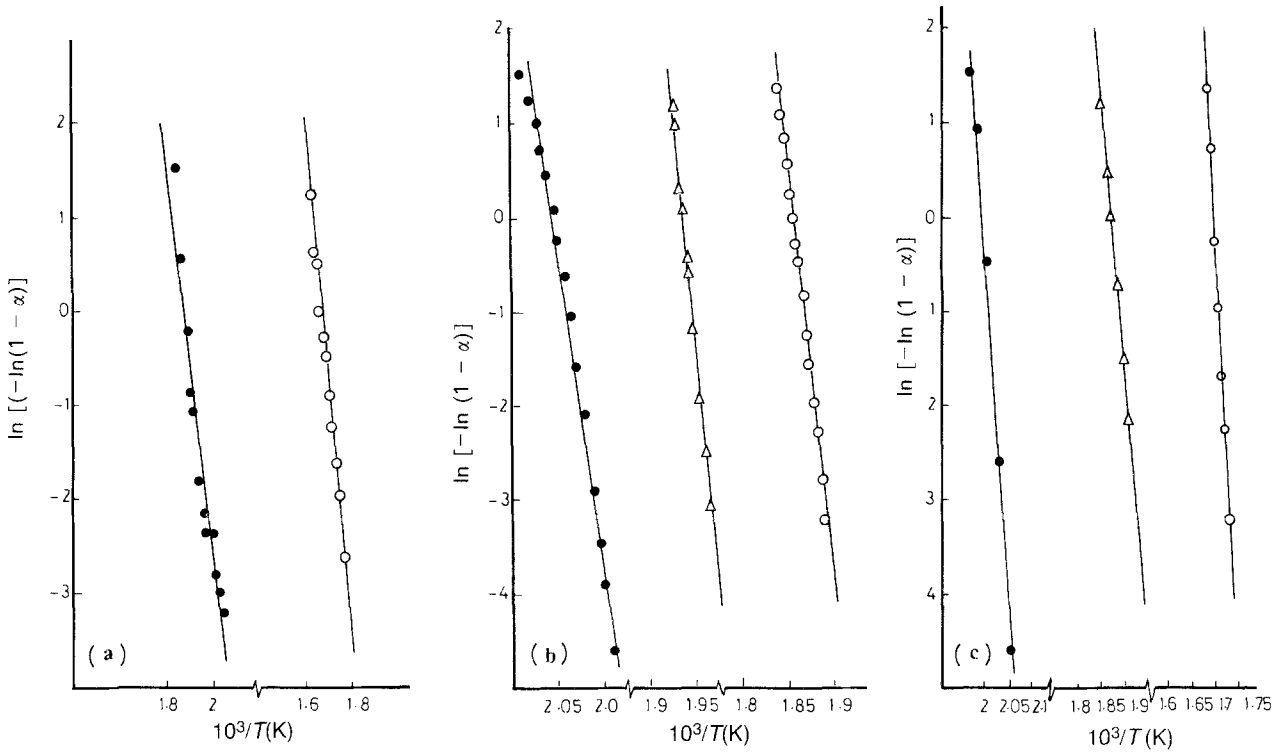

Figure 6 Plots of ln $[-\ln(1-\alpha)]$ versus $1/T$ for (●) low, (△) medium and (○) high peaks of crystallization of $Ag_x(As_2S_3)_{100-x}$, (a) $x = 6$, (b) $x = 15$ and (c) $x = 25$.

which shows that the first crystalline phase appearing in the three compositions is the same, namely that of $AgAs_2S_2$. The value of n for the composition $Ag_{25}(As_2S_3)_{75}$ decreases from 3 to 2.1 for the other two compositions. This can be explained by the structural variation of the amorphous structure base matrix, from one similar to that of As_2S_3 for low silver concentration, to one similar to $AgAs_2S_2$ for high silver concentration. This is seen in the radial distribution function analysis of X-ray diffraction from the amorphous samples [13]. The same argument can explain the low values of n (< 3) for a crystallization process (a predetermined process) for 25% silver content and the higher value of $n \gtrsim 3$ (a sporadic three-dimensional growth) for a smaller content of silver.

The relatively longest height of the first exothermic peak in the 25% silver content sample as compared to the other two peaks (Fig. 1) shows that the crystalline phase corresponding to this peak, namely $AgAs_2S_2$, is dominant. This result agrees completely with the results of X-ray diffraction studies [6]. These studies also show that traces of separated sulphur appear in the diffraction patterns. This could explain the increase in the values of E needed for formation of the crystalline phases, corresponding to the second and third peaks in the three compositions, as due to the formation of sulphur molecule boundaries hindering the crystal growth.

References

1. D. D. THORNBURG and R. I. JOHNSON, *J. Non-Cryst. Solids* **17** (1975) 2.
2. D. W. HENDERSON, *J. Non-Cryst. Solids* **30** (1979) 301.
3. M. F. KOTKATA and E. A. MAHMOUD, *Mater. Sci. Engng* **54** (1982) 163.
4. M. F. KOTKATA, M. H. EL-FOULY, A. Z. EL-BEHAY and L. A. EL-WAHAB, *ibid.* **60** (1983) 163.
5. M. F. KOTKATA, M. H. EL-FOULY, M. A. MORSY and S. A. FAYEK, *J. Non-Cryst. Solids* **97–98** (1987) 1259.
6. M. F. KOTKATA and C. S. MOHAMED, *J. Mater. Sci.* **24** (1989) 1291.
7. M. F. KOTKATA, M. M. RADWAN, F. M. METAWE and C. S. MOHAMED, *J. Non-Cryst. Solids* **77–78** (1985) 1229.
8. H. J. BORCHARD, *J. Inorg. Nucl. Chem.* **12** (1960) 252.
9. R. C. MACKENZIE, "Differential Analysis", Vol. 1 (Academic, London, 1970) p. 32.

TABLE II Crystallization kinetic parameters and melting points of the compositions investigated in the system $Ag_x(As_2S_3)_{100-x}$

Parameter	$Ag_6(As_2S_3)_{94}$		$Ag_{15}(As_2S_3)_{85}$			$Ag_{25}(As_2S_3)_{75}$		
	Low temp. peak	High temp. peak	Low temp. peak	Mid temp. peak	High temp. peak	Low temp. peak	Mid temp. peak	High temp. peak
Melting temperature, T_m (°C)	417	417	311	367	423	297	369	415
Activation energy of crystallization, E (eV)	2.45	3.1	2.7	3.3	3.6	2.4	2.6	3.25
Reaction mode, n	3	3.6	3	2.9	2.7	2.1	2.4	2.7

10. F. O. PILOYAN, I. O. RYABCHIKOV and O. S. NOVIKOVA, *Nature* **212** (1966) 1229.
11. M. F. KOTKATA and M. H. EL-FOULY, *Latin Am. J. Metall. Mater.* **5** (1985) 28.
12. J. H. SHARP, G. V. BRINDLEY and B. N. N. ACHAR, *J. Amer. Ceram. Soc.* **49** (1966) 379.
13. M. M. RADWAN, *Acta Cryst.* **A40** (1984) C476.

Received 26 July 1988
and accepted 14 April 1989